Electropolymerization of 2′-Ferrocenylpyrrolidino-[3′,4′;1,2][C_{60}]fullerene in the Presence of Palladium Acetate. Formation of an Electroactive Fullerene-Based Film with a Covalently Attached Redox Probe

Marta E. Plonska,[‡] Ana de Bettencourt-Dias,[†,§] Alan L. Balch,*[,†] and Krzysztof Winkler[‡]

Department of Chemistry, University of California, Davis, California 95616 and Institute of Chemistry, University of Bialystok, 15443 Bialystok, Poland

Received May 15, 2003. Revised Manuscript Received July 14, 2003

This article demonstrates that new redox active films can be electrochemically generated by reduction of a chemically modified fullerene (the ferrocene−fullerene conjugate 2′-ferrocenylpyrrolidino-[3′,4′;1,2][C_{60}]fullerene, Fc-C_{60}) and [$Pd(ac)_2$]$_3$. These films are electrochemically active in both positive and negative potential regions. The formation and electrochemical properties of this Fc-C_{60}/Pd film have been studied using cyclic voltammetry and electrochemical quartz crystal microbalance techniques. The surface morphology and infrared spectra of the film are also reported. At negative potentials, the electrochemical behavior of the new Fc-C_{60}/Pd film shows features similar to the ones displayed for the previously studied C_{60}/Pd film. In the positive potential range, peaks related to charge-transfer processes of the ferrocene units linked to the polymer backbone are observed. Reduction of the film at negative potentials is accompanied by transfer of cations at the solution/film interface and their transport inside the solid phase. On the other hand, the transport of the anions is involved in the process of film oxidation. The film exhibits higher permeability to the anions than to the cations. The oxidation process results in significant changes of the structure and morphology of the ferrocenylfullero[C_{60}]pyrrolidine/Pd film. Electrostatic interaction between positively charged ferrocene groups and negatively charged fullerene units within the film significantly modify the redox properties of ferrocene units. The electrochemical properties and the film structure depend also on the concentrations of the precursors in the growth solution.

Introduction

Considerable attention has been paid to the synthesis of new electroactive polymers. These materials can be used in microelectronic devices,[1−3] sensors,[4−6] polymer batteries,[9] or electrochromic devices.[10] Most of these applications are based on the phenomenon of reversible switching between conducting and insulating states by electrochemical doping/undoping of the polymer. These processes are realized via the interfacial electron and ion transfer followed by the transport of these species inside the polymer phase.[11,12] Depending on the structure of the polymer, two approaches can be applied to explain the mechanism of charge transport through the electrochemically active film.[13] In the delocalized band model, charge carriers (polarons or unpaired electrons) are delocalized over a large number of monomer units.[14,15] This model properly describes charge transport in π-conjugated systems. For redox polymers on the other hand, a chemical model of charge localized at one monomer unit is applied. In this case, the electrons or polarons are transported along the polymer chain by hopping between neighboring redox sites with different

* To whom correspondence should be addressed. Phone: 530-752-0941. Fax: 530-752-8995. E-mail: albalch@ucdavis.edu.
† University of California.
‡ University of Bialystok.
§ Present address: Department of Chemistry, Syracuse University, Syracuse, NY 13244.

(1) Chidsey, C. E. D.; Murray, R. W. *Science* **1986**, *231*, 25.
(2) Garnier, F.; Hajlaoui, R.; Yassar, A.; Srivastava, P. *Science* **1994**, *265*, 1684.
(3) Wrighton, M. S. *Science* **1986**, *231*, 32.
(4) Thackeray, J. W.; White, H. S.; Wrighton, M. S. *J. Phys. Chem.* **1985**, *89*, 5133.
(5) Fortier, G.; Brassard, E.; Belanger, D. *Biosens. Bioelectron.* **1990**, *5*, 473.
(6) Bartlett, P. N.; Whithaker, R. G. *J. Electroanal. Chem.* **1987**, *224*, 27.
(7) Gofer, Y.; Sarker, H.; Killian, J. G.; Poeher, T. O.; Searson, P. C. *Appl. Phys. Lett.* **1997**, *71*, 1582.
(8) Gofer, Y.; Sarker, H.; Killian, J. G.; Poeher, T. O.; Searson, P. C. *J. Electroanal. Chem.* **1998**, *443*, 103.
(9) Novak, P.; Muller, K.; Santhanam, K. S. V.; Haas, O. *Chem. Rev.* **1997**, *97*, 207.
(10) Yoshima, H.; Kobayashi, M.; Lee, K. B.; Chung, D.; Heeger, A. J.; Wudl, F. *J. Electrochem. Soc.* **1987**, *134*, 46.
(11) Saveant, J. M. *J. Electroanal. Chem.* **1988**, *242*, 1.
(12) Buck, R. P. *J. Phys. Chem.* **1989**, *93*, 6212.
(13) Lyons, M. E. G., Ed. *Electroactive Polymer Electrochemistry*; Plenum Press: New York, 1994; Pt. 1, Ch.1.
(14) Bredas, J. L.; Street, G. B. *Acc. Chem. Res.* **1985**, *18*, 309.
(15) Chance, R. R.; Boudreaux, D. S.; Wolf, J. F.; Shacklette, L. W.; Silbey, R.; Themans, B.; Andre, J. M.; Bredas, J. L. *Synth. Met.* **1986**, *15*, 105.

10.1021/cm034364c CCC: $25.00
Published on Web 09/09/2003

oxidation states.[16−18] Switching between oxidation states of an electroactive polymer is accompanied by ion transport and a change in polymer solvent content.[19−22] Very often ion and mass transport lead to significance changes of the polymeric phase structure.[23,24] The degree of these structural changes depends on the counterion size and its charge.

To date, most of the electroactive polymers are formed by electro-oxidation of appropriate monomers and exhibit *p*-doped properties. Polypyrrole, polyaniline, and their derivatives are the most representative examples of such materials.[25−28] However, considerable effort has been given recently to prepare and study polymers with *n*-doping properties. Electrochemically formed polythiophene exhibits such a behavior.[29−31]

Recently, we have been focusing on the electrochemical preparation of fullerene-based redox-active films and on elucidation of their properties.[32−41] Such films can be formed by the electrochemical reduction of the fullerene epoxide ($C_{60}O$),[32,33] of a mixture of C_{60} and dioxygen,[34] or of a mixture of transition metal complexes and fullerenes.[35,39] The fullerene/transition metal films are particularly interesting. In these systems, the polymeric network is believed to be formed through covalent bonding between transition metal complexes and fullerenes. Because of the presence of electron-accepting C_{60} moieties, these films exhibit *n*-doping properties. Such films can be reversibly reduced at negative potentials.[35,36] The doping process is accompanied by cation transfer from the electrolyte into the solid film on the electrode surface.[36]

Interesting properties can be expected for polymeric systems that can undergo both *p*- and *n*-doping. Generally, in these systems, the electron-accepting moieties are incorporated into an electron-donating, conjugated polymer backbone. Such "double cables" can transport both electron and holes. Recently, fullerene moieties were used in these systems as electron-accepting centers.[42−44] Both the polymeric chains and the attached fullerene groups retain their electrochemical properties. Polythiophene with pendant fullerene-containing moieties also exhibits photoinduced electron transfer from the polymeric backbone to the C_{60} acceptor moieties.[44]

In recent years, significant progress has been made in the production of stable, well-defined fullerenes adducts. The 1,3-dipolar cycloaddition of ylides to C_{60} has been frequently used to generate fullerene derivatives from a wide variety of easily accessible starting materials.[45] Using this method, a variety of different electron-donor molecules (such as tetrathiafulvalene,[46,47] ferrocene,[48−50] metalloporphyrins,[51,52] and trisbypiridineruthenium(II) complexes[53,54]) have been covalently attached to the C_{60} cage via a pyrrolidine ring. The redox properties of these molecules are a combination of the redox properties of both electroactive centers. For example, in solutions of the ferrocene−fullerene conjugate (**1**, Fc-C_{60}), 2′-ferrocenylpyrrolidino-[3′,4′;1,2][C_{60}]-fullerene, a ferrocene-centered oxidation process occurs at positive potentials, whereas in the negative potential range, the fullerene portion is reduced.[49]

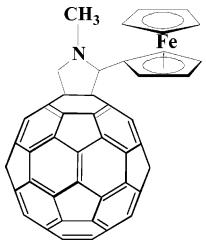

The present investigations are aimed at the study of the electropolymerization and the redox behavior of

(16) Kaufman, F. B.; Engler, E. M. *J. Am. Chem. Soc.* **1979**, *101*, 547.
(17) Kaufman, F. B.; Schroeder, A. H.; Engler, E. M.; Kramer, S. R.; Chambers, J. Q. *J. Am. Chem. Soc.* **1980**, *102*, 483.
(18) Bockris, J. O'M.; Dinz, F. B. *Electrochim. Acta* **1989**, *34*, 567.
(19) Paulse, C. D.; Pickup, P. G. *J. Phys. Chem.* **1988**, *92*, 7002.
(20) Aoki, K.; Tezuka, Y. *J. Electroanal. Chem.* **1989**, *267*, 55.
(21) Hillman, A. R.; Swann, M. J.; Bruckenstein, S. *J. Electroanal. Chem.* **1990**, *291*, 147.
(22) Nyffenegger, R.; Ammann, E.; Sigenthaler, H.; Kotz, R.; Haas, O. *Electrochim. Acta* **1995**, *40*, 1411.
(23) Heinze, J.; Bilgr, R.; Meerholz, K. *Ber. Bunsen-Ges. Ohys. Chem.* **1988**, *92*, 1266.
(24) Otero, T. F.; Grande, H.; Rodriguez, J. *Synth. Met.* **1997**, *85*, 1077.
(25) Diaz, A. F.; Castillo, J. I.; Logan, J. A.; Lee, W.-Y. *J. Electroanal. Chem.* **1981**, *129*, 115.
(26) Fermin, D. J.; Teruel, H.; Scharifker, B. R. *J. Electroanal. Chem.* **1996**, *401*, 207.
(27) Rubinstein, I.; Sabatani, E.; Rishpon, J. *J. Electrochem. Soc.* **1987**, *134*, 3078.
(28) Genies, E. M.; Tsintavis, C. *J. Electroanal. Chem.* **1985**, *195*, 109.
(29) Kaneto, K.; Yoshino, K.; Inuishi, J. *Jpn. J. Appl. Phys.* **1983**, *22*, 567.
(30) Ferraris, J. P.; Eissa, M. M.; Brotherston, I. D.; Loveday, D. C.; Moxry, A. A. *J. Electroanal. Chem.* **1998**, *459*, 57.
(31) Mastragostino, M.; Soddu, L. *Electrochim. Acta* **1990**, *35*, 463.
(32) Fedurco, M.; Costa, D. A.; Balch, A. L.; Fawcett, W. R. *Angew. Chem., Int. Ed. Engl.* **1995**, *34*, 194.
(33) Winkler, K.; Costa, D. A.; Balch, A. L.; Fawcett, W. R. *J. Phys. Chem.* **1995**, *99*, 17431.
(34) Winkler, K.; Costa, D. A.; Fawcett, W. R.; Balch, A. L. *Adv. Mater.* **1997**, *9*, 153.
(35) Balch, A. L.; Costa, D. A.; Winkler, K. *J. Am. Chem.* Soc. **1998**, *120*, 9614.
(36) Winkler, K.; de Bettencourt-Dias, A.; Balch, A. L. *Chem. Mater.* **1999**, *11*, 2265.
(37) Winkler, K.; Noworyta, K.; Kutner, W.; Balch, A. L. *J. Electrochem. Soc.* **2000**, *147*, 2597.
(38) Winkler, K.; de Bettencourt-Dias, A.; Balch, A. L. *Chem. Mater.* **2000**, *12*, 1386.
(39) Hayashi, A.; de Bettencourt-Dias, A.; Winkler, K.; Balch, A. L. *J. Mater. Chem.* **2002**, *12*, 2116.
(40) Winkler, K.; Brumas, A.; Noworyta, K.; Sobczak, J. W.; Wu, C.-T.; Chen, L.-C.; Kutner, W.; Balch, A. L. *J. Mater. Chem.* **2003**, *13*, 518.
(41) Winkler, K.; de Bettencourt-Dias, A.; Balch, A. L.; Fawcett, W. R. *J. Electroanal. Chem.* **2003**, *549*, 109.
(42) Anderson, H. L.; Boudou, C.; Diederich, F.; Gisselbrecht, J.-P.; Gross, M.; Seiler, P. *Angew. Chem., Int. Ed. Engl.* **1994**, *33*, 1628.
(43) Benincori, T.; Brenna, E.; Sannicolo, F.; Trimarco, L.; Zoti, G.; Sozzani, P. *Angew. Chem., Int. Ed. Engl.* **1996**, *35*, 648.
(44) Cravino, A.; Zerza, G.; Neugebauer, H.; Maggini, M.; Bucella, S.; Menna, E.; Svensson, M.; Andersson, M. R.; Brabec, C. J.; Sariciftci, N. S. *J. Phys. Chem. B* **2002**, *106*, 70.
(45) Prato, M.; Maggini, M. *Acc. Chem. Res.* **1998**, *31*, 519.
(46) Herrans, M. A.; Illescas, B.; Martin, N.; Luo, C.; Guldi, D. M. *J. Org. Chem.* **2000**, *65*, 5728.
(47) Herrans, M. A.; Martin, N.; Sanchez, L.; Seoane, C.; Guldi, D. M. *J. Organomet. Chem.* **2000**, *599*, 2.
(48) Maggini, M.; Karlsson, A.; Scorrano, G.; Sandona, G.; Farnia, G.; Prato, M. *J. Chem. Soc., Chem. Commun.* **1994**, 589.
(49) Prato, M.; Maggini, M.; Giacometti, C.; Scorrano, G.; Sandona, G.; Farnia, G. *Tetrahedron* **1996**, *52*, 5221.
(50) Guldi, D. M.; Maggini, M.; Scorrano, G.; Prato, M. *J. Am. Chem. Soc.* **1997**, *119*, 974.
(51) Kuciauskas, D.; Lin, S.; Seely, G. R.; Moore, A. L.; Moore, T. A.; Gust, D.; Drovetskaya, T.; Reed, C. A.; Boyd, P. D. W. *J. Phys. Chem.* **1996**, *100*, 15926.
(52) Akiyama, T.; Imahori, H.; Ajawakom, A.; Sakata, Y. *Chem. Lett.* **1996**, 907.
(53) Maggini, M.; Dono, A.; Scorrano, G.; Prato, M. *J. Chem. Soc., Chem. Commun.* **1995**, 845.
(54) Sariciftci, N. S.; Wudl, F.; Heeger, A. J.; Maggini, M.; Scorrano, G.; Prato, M.; Bourassa, J.; Ford, P. C. *Chem. Phys. Lett.* **1995**, *247*, 210.

ferrocenylfullero[C_{60}]pyrrolidine/Pd films. The aim of the work is the creation of a new redox-active fullerene-based polymer with both *p*- and *n*-doping properties due to the presence of both electron-donating ferrocene and electron-accepting fullerene moieties. In this case, the C_{60} portion and Pd atoms form a polymeric backbone with ferrocene centers covalently linked to it. Characterization of the film was done by cyclic voltammetry, electrochemical quartz crystal microbalance studies, FT-IR spectroscopy, and scanning electron microscopy.

Experimental Section

Materials. 2′-Ferrocenylpyrrolidino-[3′,4′;1,2][C_{60}]fullerene was synthesized according to a method described in the literature.[49,55] Ferrocene carboxyaldehyde, *N*-methylglycine, and palladium(II) acetate trimer, [$Pd(ac)_2]_3$, (Aldrich) and C_{60} (Southern Chemical Group) were used as received. The following supporting electrolytes were dried under vacuum for 24 h prior to use: tetra(*n*-butyl)ammonium perchlorate (TBAClO_4, Sigma Chemical Co.), tetra(*n*-butyl)ammonium tetrafluoroborate (TBABF_4, Sigma), tetra(*n*-butyl)ammonium tetraphenylborate (TBABPh_4, Sigma), tetra(*n*-hexyl)ammonium perchlorate (THxAClO_4, Fluka), tetra(ethyl)ammonium perchlorate (TEAClO_4, Fluka). Acetonitrile (99.9%, Aldrich Chemical Co.) was used as received. Toluene (Aldrich) was purified by distillation over sodium under a dinitrogen atmosphere.

Instrumentation. Voltammetric experiments were performed on an EG&G Instruments model 283 potentiostat/galvanostat with a three-electrode cell. A gold disk with a diameter of 1.5 mm (Bioanalytical Systems Inc.) was used as working electrode. Prior to the experiment, the electrode was polished with fine carborundum paper and then with a 0.5-μm alumina slurry. Subsequently, the electrode was sonicated in water to remove traces of alumina from the gold surface, washed with water, and dried. A silver wire immersed in 0.010 M silver perchlorate and 0.090 M tetra(*n*-butyl)ammonium perchlorate in acetonitrile served as the reference electrode. The reference electrode was separated from the working electrode by a ceramic tip (Bioanalytical Systems Inc.). The counter electrode was a platinum tab with an area of about 0.5 cm^2.

Simultaneous voltammetric and piezoelectric microgravimetry experiments were carried out with a home-built potentiostat and electrochemical quartz crystal microbalance, EQCM 5510, of the Institute of Physical Chemistry (Warsaw, Poland). Because plano−convex quartz crystals confine acoustic energy to the center of the crystal much better than the plano−plano crystals,[56] the former were used. The 14-mm-diameter AT-cut, plano−convex quartz crystals of the 5 MHz resonant frequencies were obtained from Omig (Warsaw, Poland). A 100-nm gold film that was vacuum deposited on the quartz crystal served as the working electrode. The projected area of this Au electrode, which included a 5-mm- diameter center spot and two contacting radial strips, was 0.24 cm^2. Unpolished quartz crystals were used for better adherence of the film. The sensitivity of the mass measurement calculated from the Saurbrey equation was ±17.7 ng Hz^{-1} cm^{-2}.

The FT-IR spectra were recorded using a Magna IR 550 Series II spectrometer. A spectral resolution of 4 cm^{-1} was used.

Scanning electron micrograph (SEM) images were obtained with the use of a LEO 435 vp microscope. The accelerating voltage of the electron beam was 15 kV.

Results

Film Growth Procedure and Electroactivity Studies. Ferrocenylfullereno[C_{60}]- pyrrolidine/Pd films were prepared typically through electroreduction of an acetonitrile/toluene (1:4, v:v) solution that contained both ferrocenylfullereno[C_{60}]-pyrrolidine and palladium(II) acetate trimer, and the supporting electrolyte, 0.10 M TBAClO_4. Films were grown under cyclic voltammetry conditions at a sweep rate of 100 mV/s. The electrochemical properties of the ferrocenylfullereno[C_{60}]-pyrrolidine/Pd film were studied in acetonitrile solution containing only the supporting electrolyte. In this case, the electrode covered with the film was rinsed several times with acetonitrile/toluene (1:4, v:v) solution and then placed in an acetonitrile solution containing 0.10 M of supporting electrolyte. The transfer of the electrode from one solvent to another was accomplished in air without protection from normal atmospheric conditions. The modified electrode was allowed to equilibrate for 10 min while degassing in the new solution before electrochemical measurements were conducted.

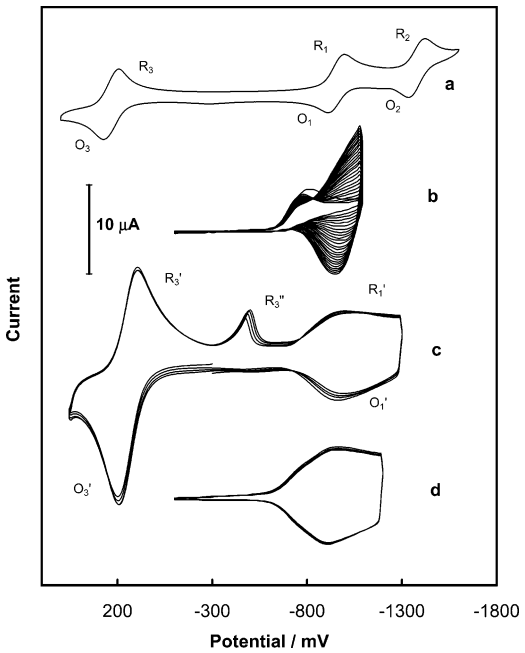

Figure 1. (a) Cyclic voltammograms obtained for 0.31 mM Fc-C_{60} (**1**) in acetonitrile/toluene (1:4, v:v) containing 0.10 M TBAClO_4. (b) Multicyclic voltammogram (20 cycles) obtained for 0.31 mM Fc-C_{60} (**1**) and 0.55 mM [$Pd(ac)_2]_3$ in acetonitrile/toluene (1:4, v:v) containing 0.10 M TBAClO_4. (c) Multicyclic voltammogram (4 cycles) of Fc-C_{60}/Pd electropolymerized film over the potential range from +500 to −1300 mV in acetonitrile containing 0.10 M TBAClO_4. The film was obtained from 0.31 mM Fc-C_{60} (**1**) and 0.55 mM [$Pd(ac)_2]_3$ in acetonitrile/toluene (1:4, v:v) containing 0.10 M TBAClO_4. (d) Multicyclic voltammogram (4 cycles) of Fc-C_{60}/Pd film over the potential range from −100 to −1250 mV in acetonitrile containing 0.10 M TBAClO_4. The film was obtained from 0.31 mM Fc-C_{60} (**1**) and 0.55 mM [$Pd(ac)_2]_3$ in acetonitrile/toluene (1:4, v:v) containing 0.10 M TBAClO_4. The sweep rate was 100 mV s^{-1}.

Electropolymerization of 2′-Ferrocenylpyrrolidino-[3′,4′;1,2][C_{60}]fullerene (1) in the Presence of Palladium Acetate Trimer. The voltammogram of acetonitrile/toluene (1:4, v:v) solution containing (**1**) and 0.10 M tetra(*n*-butyl)ammonium perchlorate seen in Figure 1a shows two reversible, reduction peaks (R_1 and R_2) of the fullerene moiety at −800 and −1150 mV. The reversible oxidation of the ferrocene moiety is seen at +200 mV (O_3). This behavior is analogous to the data previously presented in the literature.[49] Trace b of Figure 1 was recorded in a solution that contained (**1**)

(55) Prato, M.; Maggini, M.; Scorrano, G. *Synth. Met.* **1996**, *77*, 89.
(56) Hiller, A. C.; Ward, M. D. *Anal. Chem.* **1992**, *64*, 2539.

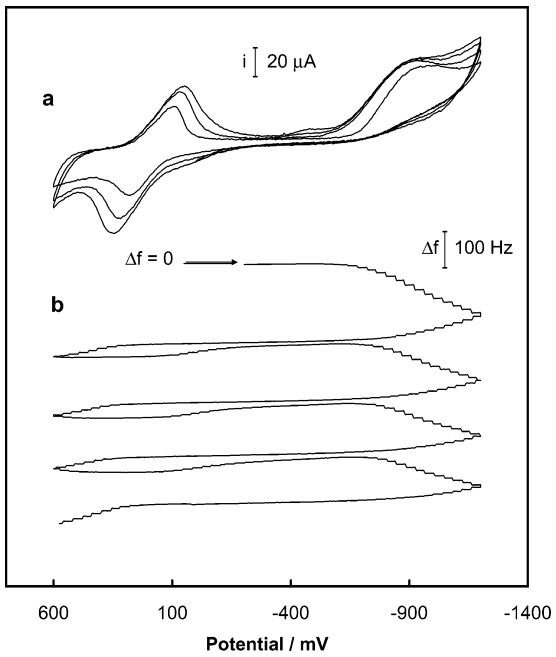

Figure 2. Simultaneously recorded at the same Au/quartz electrode multicyclic voltammograms (a) and (b) curves of frequency change vs potential for 0.31 mM Fc-C_{60} (**1**) and 0.55 mM $[Pd(ac)_2]_3$ in acetonitrile/toluene (1:4, v:v) containing 0.10 M $TBAClO_4$. The sweep rate was 100 mV s^{-1}.

and palladium(II) acetate trimer. Upon repeated scanning of the potential between +200 and −1200 mV, an increase of current in the potential range for reduction of the fullerene moiety is seen. Examination of the electrode surface after multicyclic potential scanning reveals the presence of a black deposit of Fc-C_{60}/Pd.

The formation of the Fc-C_{60}/Pd film has been also studied using EQCM. In Figure 2, multicyclic voltammograms and curves of changes of resonant frequency, Δf, vs. potential are presented. These data were recorded simultaneously at an Au/quartz electrode. The differences between voltammograms presented in Figure 1b and 2a are due to the fact that ohmic drop has not been compensated in the EQCM experiment. The deposition of the film is clearly apparent from the mass increase (frequency decrease) at negative potentials (Figure 2b). The frequency changes in the positive potential range are related to the oxidation/reduction processes of ferrocene moieties within the film, which are accompanied by ion transport between the film and the solution.

The infrared spectrum obtained by the horizontal attenuated total reflectance (HATR) method from the Fc-C_{60}/Pd film is shown in traces d and e of Figure 3. For comparison the spectra of the C_{60}/Pd film obtained by the (HATR) method is shown in trace b and the infrared spectra of ferrocene and C_{60}, obtained from KBr pellets, are shown in traces c and a, respectively. The spectra of the Fc-C_{60}/Pd and the C_{60}/Pd films show similar features, but as expected the spectrum of the Fc-C_{60}/Pd film is more complex. Significantly, the Fc-C_{60}/Pd film exhibits absorption bands at 821, 998, and 1104 cm^{-1} that are due to the presence of the ferrocene unit within the film.

Electrochemical Properties of Fc-C_{60} Films. The electrode coated with the black Fc-C_{60}/Pd film retains its redox activity both in negative and positive potential

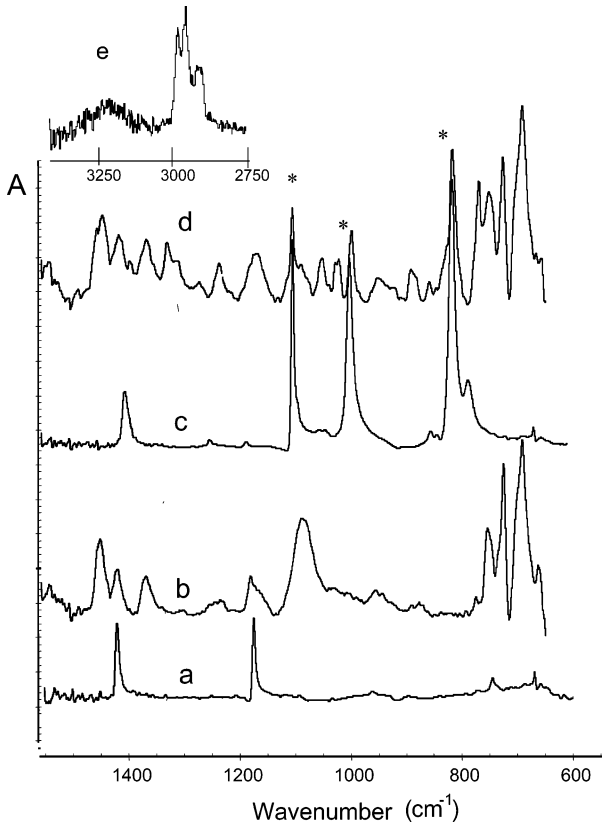

Figure 3. Infrared spectra of (a) C_{60} in a KBr pellet, (b) C_{60}/Pd film obtained by the (HATR) method, (c) ferrocene in a KBr pellet, and (d) and (e) Fc-C_{60}/Pd film obtained by the (HATR) method.

ranges when it is transferred to a solution of acetonitrile that contains only the supporting electrolyte, 0.10 M tetra(*n*-butyl)ammonium perchlorate. Relevant data are shown in trace c of Figure 1. The broad peaks R_1' and O_1' have been also observed for C_{60}/Pd[35−38] and C_{60}/Pt films.[39] These peaks are related to the reduction and reoxidation of fullerene moieties in the film. The oxidation peak O_3' and a pair of reduction peaks, R_3' at ca. +100 mV and R_3'' at ca. −600 mV are due to the process of ferrocene oxidation. If the anodic switching potential is less positive than the potential of ferrocene oxidation, the R_3'' peak is not observed as seen in Figure 1d. The charge related to the reduction of the C_{60} moieties, $Q_{R1'}$, is equal to the charge of the respective oxidation process, $Q_{O1'}$. For the processes of ferrocene oxidation in the positive potential range, the charge of the oxidation process, $Q_{O3'}$, is equal to the sum of the charges for the two reduction processes $Q_{R3'}$ and $Q_{R3''}$. This indicates that the additional small and sharp R_3'' peak is related to the reduction of positively charged ferrocene groups. It also has to be stressed that the charge for the ferrocene oxidation is significantly higher than the charge of reduction of the fullerene portion.

The difference between anodic and cathodic peak potentials as a function of sweep rate was also investigated for both processes. The relevant data are presented in Figure 4. For a reversible, surface charge-transfer process, the potentials of the anodic and cathodic peaks are the same.[57,58] For the process of C_{60} group reduction, a small departure from the theoreti-

(57) Murray, R. W., Ed. *Molecular Design of Electrode Surfaces*; J. Wiley and Sons: New York, 1992; pp 1−48.

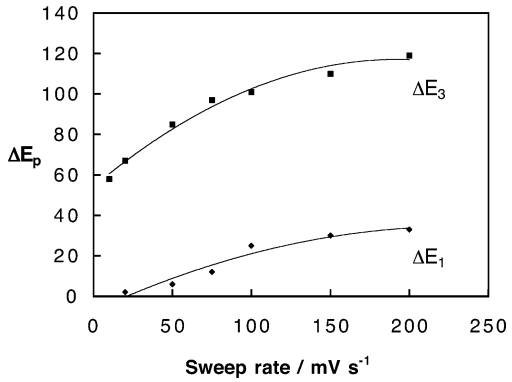

Figure 4. Dependence of the difference between cathodic and anodic peak potentials for fullerene (ΔE_1) and ferrocene (ΔE_2) electrode processes on the sweep rate in acetonitrile containing 0.10 M $TBAClO_4$. The film was electropolymerized under cyclic voltammetry conditions (20 cycles) from 0.31 mM Fc-C_{60} and 0.55 mM $[Pd(ac)_2]_3$ in acetonitrile/toluene (1:4, v:v) containing 0.10 M $TBAClO_4$.

cally predicted behavior is observed. In this case, the difference between the cathodic and anodic peak potentials is likely due to the partially uncompensated resistance. However, for the process of ferrocene oxidation, the separation between the anodic (O_3') and the cathodic (R_3') peak potentials is much higher. It was also observed that the potential of the cathodic peak is practically independent of the sweep rate. The increase of ΔE_3 with an increase in sweep rate shown in Figure 4 is due to the strong effect of the sweep rate on the oxidation peak, O_3', potential. These results strongly indicate that the process of Fc-C_{60}/Pd film oxidation is accompanied by substantial structural changes.

In Figure 5 the surface morphologies of films formed under cyclic voltammetry conditions in the potential range from −200 to −1200 mV (panel a) and from +500 to −1200 mV (panel b) are shown. The SEM images in Figure 5 show that both films grow to a uniform thickness. The surface morphology of an electrochemically formed Fc-C_{60}/Pd is similar to the one observed for the C_{60}/Pd film.[35,41] The film formed in the potential range from −200 to −1200 mV is relatively flat with a few outcroppings. However, if in the anodic scan the potential reaches values of ferrocene oxidation potentials, the film formed on the electrode surface is more porous.

The changes in the structure of the film at positive potentials influence the electrochemical properties and stability of the film. This film was formed under cyclic voltammetry conditions in the potential range from −200 to −1200 mV and then transferred to an acetonitrile solution containing $TBAClO_4$. In the acetonitrile solution, the film exhibits a stable reversible response over the −200 to −1600 mV range as seen in trace a in Figure 6. The decomposition of the film was observed at potentials more negative than about −1800 mV as seen in trace b of Figure 6. For the first few cycles in this potential range, stable electrochemical behavior was observed. Subsequently, the film reduction potential shifts toward more negative values and a decrease of the oxidation charge is observed. Traces c and d of Figure 6 show the voltammetric response of the film in acetonitrile in the potential range from +500 mV to −1600 mV, and from +500 mV to −2000 mV, respectively. Small changes of the current in the potential range of ferrocene oxidation are observed on trace c. However, after a few initial cycles the voltammetric response of the film stabilizes. As seen in trace d of Figure 6, film cycled over the potential range from +500 to −2000 quickly loses its electrochemical activity. The oxidation current for the film at positive potentials practically drops to zero in the second cycle. A decrease of film reduction current at negative potentials in the subsequent cycles is also observed. This effect is caused by the loss of redox active material from the surface, which can be observed visually. The film instability is likely to result from the strong repulsion interactions between the multiply negatively charged C_{60} units that are formed upon film reduction, and the mechanical strain produced by the influx of cations as discussed previously.[38]

The effect of the thickness of the film on its voltammetric response has been also investigated. The relevant data are shown in Figure 7. The amount of Fc-C_{60}/Pd film deposited was controlled by the number of voltammetric cycles used for film deposition as was done previously for the C_{60}/Pd film.[36] The process of polymer reduction at negative potentials is almost independent of the film thickness. The reduction, R_1', and oxidation, O_1', currents increase due to the increase in the amount of electroactive material on the electrode surface. However, the peak potentials and the shapes of the peaks are not affected by the thickness of the layer. More complex behavior was observed for the ferrocene-involving film oxidation process. For thin layers, both O_3' and R_3' peaks exhibit a characteristic symmetric bell shape. The separation of about 50 mV between anodic and cathodic peak potential is observed, but both peak potentials are constant. For thicker films, the shift of the anodic O_2' peak toward more positive potentials with an increase in the film thickness is observed. The potential of the reduction peak remains almost the same. Both peaks also exhibit diffusional tailing in the current at potentials following the peak. The effect of film thickness and the effect of the sweep rate described earlier in this paper on the electrochemical properties of Fc-C_{60}/Pd film are very similar and indicate a change in the mechanism of charge transfer through the layer. It is also intriguing that, for thin films, the R_3''peak is not present in the voltammograms.

Effects of the Supporting Electrolyte on the Electrochemical Properties of Fc-C_{60}/Pd Films. Figure 8 shows simultaneously recorded voltammograms and frequency changes as a function of potential for an electrode covered with Fc-C_{60}/Pd in an acetonitrile solution containing only $TBAClO_4$. The decrease of frequency in the potential ranges of film reduction and oxidation are related to the mass changes due to counterion incorporation into the film in order to maintain charge neutrality. For the fullerene-involving charge-transfer process, the frequency quickly reaches its initial value in the positive scan due to the reversible charging/discharging of the film. In the case of ferrocene-involving charge-transfer process, two potential ranges of frequency change corresponding to the R_3' and

(58) Bartlett, P. N. In *Biosensors*: *Fundamentals and Applications*; Turner, A. P. F., Karube, I., Wilson, G. S., Eds.; Oxford University Press: New York, 1987; pp 211−246.

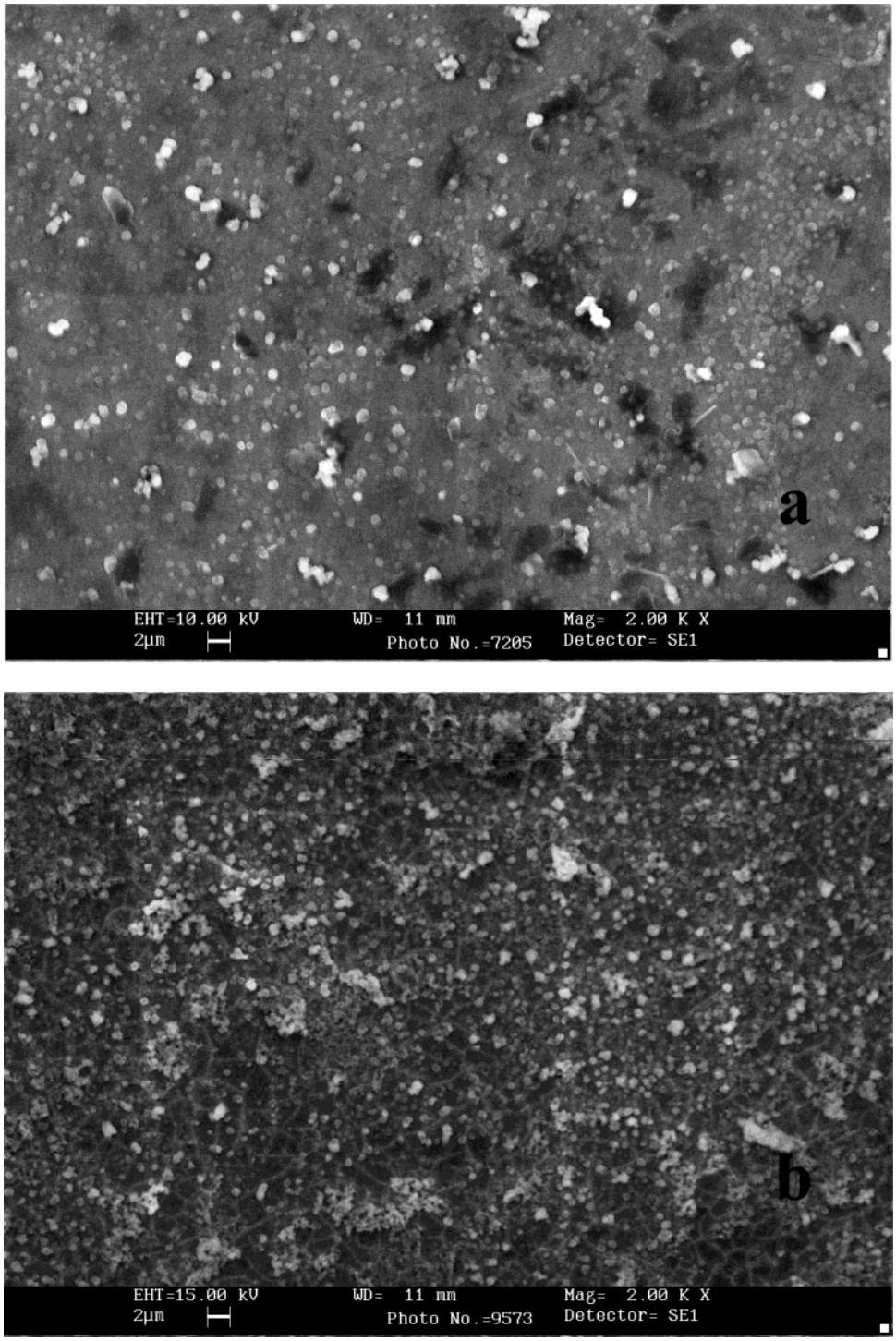

Figure 5. SEM images of films formed on gold foil under cyclic voltammetry conditions (20 cycles) from 0.31 mM Fc-C_{60} (**1**) and 0.55 mM $[Pd(ac)_2]_3$ in acetonitrile/toluene (1:4, v:v) containing 0.10 M $TBAClO_4$ cycled (10 cycles) over the potential range from −200 to −1200 mV (a) and +500 to −1200 (mV) (b). The sweep rate was 100 mV s^{-1}.

R_3'' peaks are observed. This once again indicates strongly that the R_3'' peak is related to the process of ferrocene group oxidation in the anodic scan.

Comparison of the total charge for film reduction (Q = 148 μC) with the respective mass change of the quartz resonator (302 ng) allows us to calculate the molar mass of the ions transferred from the solution into the film. Thus we calculated the mass to be 197 amu. This value is somewhat lower than that expected for TBA^+ (242 amu). However, the charge is overestimated because of the large capacitance charge contribution. On the other hand, the mass calculated for the film oxidation process (Q = 185 μC, and mass = 370 ng) is equal to 192 amu. This value is too high in comparison to the mass of perchlorate ion (99.5 amu). This discrepancy suggests that the transfer of small anions is accompanied by the transport of solvent into the film.

Figure 9 shows the effect of different cations of the supporting electrolyte on the electrochemical properties of the Fc-C_{60}/Pd film. The film was formed under cyclic voltammetry conditions in the potential range from +200 to −1200 mV and then transferred to the acetonitrile solution containing different tetra(*n*-alkyl)ammonium perchlorate salts. In this case, only the fullerene-

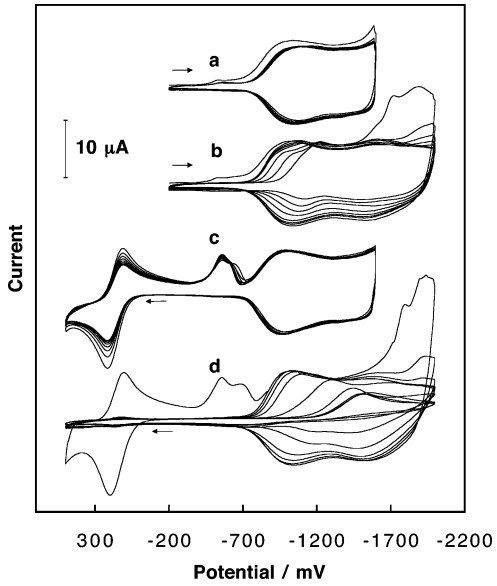

Figure 6. Multicyclic voltammogram (10 cycles) of electropolymerized Fc-C_{60}/Pd film over the potential ranges from −200 to −1600 mV (a), −200 to −2000 mV (b), +500 to −1600 mV (c), and +500 to −2000 mV (d) in acetonitrile containing 0.10 M $TBAClO_4$. The film was obtained from 0.31 mM Fc-C_{60} (**1**) and 0.55 mM $[Pd(ac)_2]_3$ in acetonitrile/toluene (1:4, v:v) containing 0.10 M $TBAClO_4$. The sweep rate was 100 mV s^{-1}.

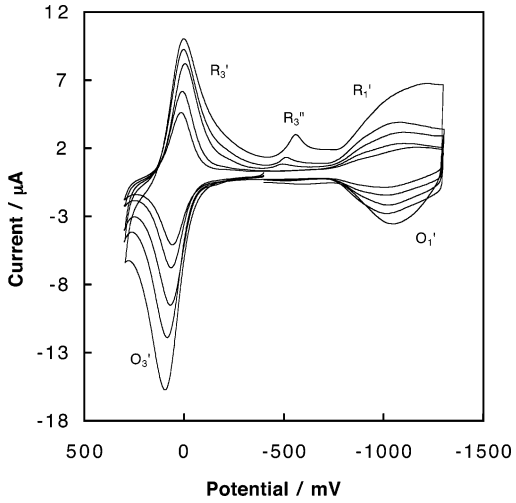

Figure 7. Cyclic voltammogram of Fc-C_{60}/Pd films in acetonitrile containing 0.10 M $TBAClO_4$. Films were obtained under cyclic voltammetry conditions (4, 8, 16, 30, and 50 cycles) from 0.31 mM Fc-C_{60} (**1**) and 0.55 mM $[Pd(ac)_2]_3$ in acetonitrile/toluene (1:4, v:v) containing 0.10 M $TBAClO_4$. The sweep rate was 100 mV s^{-1}.

involving charge transfer processes at negative potentials are affected. Reduction and reoxidation of the film increases with a decrease in the size of cation. However, the fullerene-involved charge transfer processes remain reversible for all studied cations. The ratio of oxidation to reduction charge is close to 1, and the cathodic and anodic parts of the voltammogram are almost symmetrical in the negative potential range. On the other hand, the process of film reduction at negative potentials shows insignificant alterations with the changes of the supporting electrolyte anion as shown in Figure 10. However, the ferrocene-centered electrode processes do depend on the size of the anion of the supporting electrolyte. Only small differences in charge related to film oxidation were observed for perchlorate and tetrafluoroborate ions due to the similar size of both anions. A significance decrease of oxidation charge is recorded for the larger tetraphenylborate ion. In this case, the ferrocene-involved oxidation process also becomes less reversible.

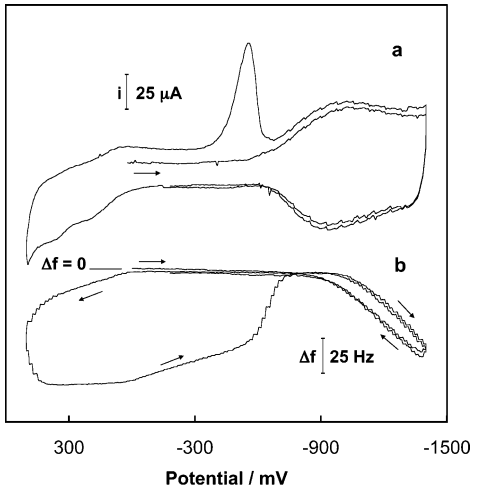

Figure 8. Multicyclic voltammograms (a) and curves of frequency charge vs potential (b) simultaneously recorded at the same Au/quartz electrode coated with Fc-C_{60}/Pd film with acetonitrile containing 0.10 M $TBAClO_4$. The sweep rate was 100 mVs^{-1}. The film was formed under cyclic voltammery conditions (20 cycles) from 0.31 mM Fc-C_{60} (**1**) and 0.55 mM $[Pd(ac)_2]_3$ in acetonitrile/toluene (1:4, v:v) containing 0.10 M $TBAClO_4$.

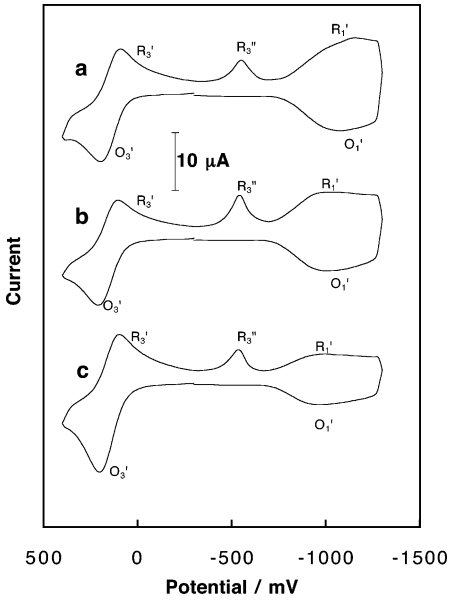

Figure 9. Cyclic voltammograms of Fc-C_{60} /Pd film over the potential range from +500 to −1300 mV in acetonitrile containing 0.10 M $TEAClO_4$ (a), $TBAClO_4$ (b), and $THxAClO_4$ (c). The film was obtained from 0.31 mM Fc-C_{60} (**1**) and 0.55 mM $[Pd(ac)_2]_3$ in acetonitrile/toluene (1:4, v:v) containing 0.10 M $TBAClO_4$. The sweep rate was 100 mV s^{-1}.

Effect of [Pd]/[Fc-C_{60}] Ratio in the Growth Solution on the Electrochemical Properties of the Fc-C_{60}/Pd Film. In the case of electrochemically grown C_{60}/Pd films, two parallel processes occur at the electrode surface that must be considered: the formation of $(-PdC_{60}-)_n$ chains, and palladium nanocluster deposition. Palladium nanoclusters have been detected in C_{60}/Pd films through high-resolution transmission electron microscopy and selected area diffraction studies and

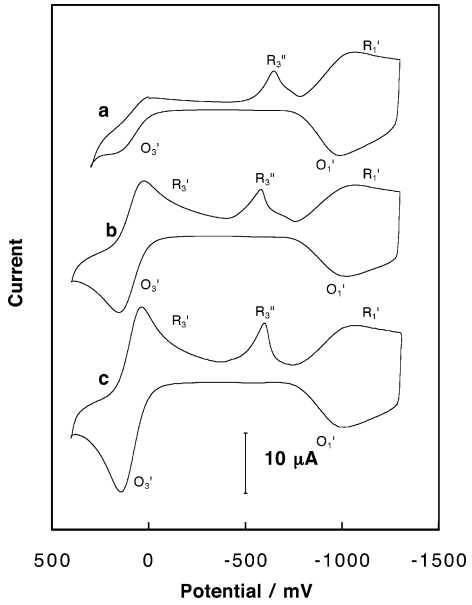

Figure 10. Cyclic voltammograms of Fc-C_{60}/Pd film over the potential range from +500 to −1300 mV in acetonitrile containing 0.10 M $TBABPh_4$ (a), $TBAClO_4$ (b), and $TBABF_4$ (c). The film was obtained from 0.31 mM Fc-C_{60} (**1**) and 0.55 mM $[Pd(ac)_2]_3$ in acetonitrile/toluene (1:4, v:v) containing 0.10 M $TBAClO_4$. The sweep rate was 100 mV s^{-1}.

through the observation of catalytic hydrogen evolution during electrochemical cycling in aqueous acid.[37,40] Since the methods of film preparation for both the C_{60}/Pd and the Fc-C_{60}/Pd films are the same, we expect that palladium nanoclusters are also present in the Fc-C_{60}/Pd film. Because the yields of both processes depend on the solution composition, redox properties of the film are also affected by the relative concentration of palladium complex and fullerene in the solution.

In contrast to C_{60}/Pd films,[40] the morphology of the films formed in solution with a relatively high concentration of $[Pd(ac)_2]_3$ (1.31 mM) does not differ significantly from the structure of Fc-C_{60}/Pd layers produced in a solution with lower concentration of palladium complex (Figure 5). The surface of the film is relatively flat with uniformly distributed porous grains.

Cyclic voltammograms for the electrodes coated with Fc-C_{60}/Pd grown in solutions with varying ratios of the film precursors and transferred to a 0.10 M $TBAClO_4$ acetonitrile solution are presented in Figure 11. An increase of $[Pd(ac)_2]_3$ concentration in the growth solution results in an increase in the reversibility of the ferrocene-centered charge-transfer process at positive potentials. For a film-forming solution containing 1.1 mM $[Pd(ac)_2]_3$, peaks R_3' and O_3' became symmetrical with a relatively low (about 40 mV) difference between the cathodic and anodic peak potentials as seen in Figure 11a. The small R_3'' peak is not observed in this case in the voltammograms. For films formed in a solution with a lower $[Pd(ac)_2]_3$ concentration, peaks recorded at positive potentials show diffusional tailing and much higher separation between the anodic O_3' and cathodic R_3' peaks, as can be seen in Figure 11c. Results presented in Figure 11 also show that the charge of oxidation of the film formed in solution with high palladium complex concentration is relatively low in comparison to the one observed for films grown in solutions containing lower amounts of $[Pd(ac)_2]_3$.

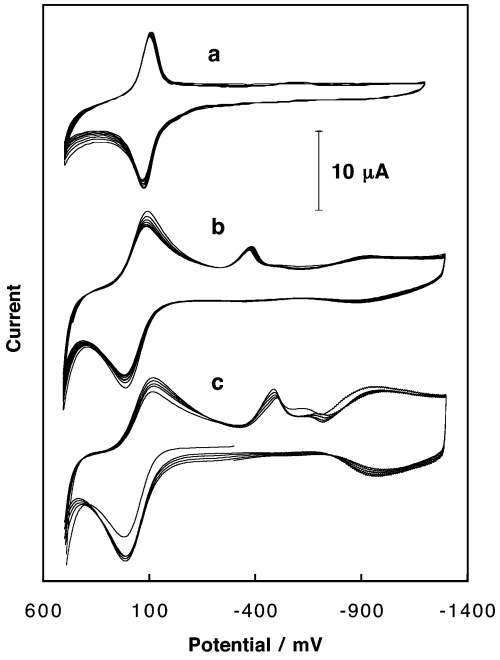

Figure 11. Multicyclic voltammogram (10 cycles) of Fc-C_{60}/Pd film over the potential range from +500 to −1250 mV in acetonitrile containing 0.10 M $TBAClO_4$. The film was obtained under cyclic voltammetry conditions from 0.31 mM Fc-C_{60} (**1**) and 1.1 mM (a), 0.83 mM (b), and 0.55 mM (c) $[Pd(ac)_2]_3$ in acetonitrile/toluene (1:4, v:v) containing 0.10 M $TBAClO_4$. The sweep rate was 100 mV s^{-1}.

A significant effect of the Fc-C_{60}/[Pd] ratio on the redox behavior of the film at negative potentials is also observed. The charge corresponding to R_1' and O_1' peaks decreases with increase of the $[Pd(ac)_2]_3$ concentration in the growth solution. The data in Figure 11 show that films formed in solution containing 1.1 mM palladium(II) acetate trimer do not show any electrochemical activity in the negative potential range. However, the HATR spectra of these films reveal features similar to those shown in trace d of Figure 3 and indicate that the fullerene moieties are present in the film.

Discussion

A new electroactive film has been prepared by electroreduction of mixtures of Fc-C_{60} (**1**) with $[Pd(ac)_2]_3$ in toluene/acetonitrile solution. Thus, this work demonstrates that chemically modified fullerenes can be used to deposit redox active films when reduced in the presence of $[Pd(ac)_2]_3$. The presence of a fairly large appendage on the fullerene does not interrupt the electropolymerization process, and other chemically modified fullerenes may also form related redox active films. The resulting "double-cable" Fc-C_{60}/Pd polymer differs from other electropolymerized ($p-n$) type polymers containing pendant fullerene moieties,[42−44] in that fullerene moieties form part of the polymer backbone and the electron-accepting ferrocene groups are covalently linked to it. The mechanism of this film formation is similar to the one described earlier for C_{60}/Pd film formation.[37] The polymer deposition is initiated by the reduction of Pd(II) to Pd(0). Pd(0) forms an intermediate complex with Fc-C_{60}. This complex may both initiate the growth of the $(-C_{60}Pd-)_n$ polymeric chain or decompose to palladium nanoclusters.[37] The

yield of each process depends on the concentration ratio of film formation precursors in solution. Therefore, the film's electrochemical properties are strongly affected by the composition of growth solution.

The electrode covered with the Fc-C_{60}/Pd film exhibits electrochemical activity both at negative and positive potentials. The reduction of the film at negative potentials is due to the presence of fullerene centers in the main polymeric chain and resembles that of the C_{60}/Pd film.[35,36] Switching between oxidation states at negative potentials under voltammetric conditions results in broad peaks with high capacity current. Such behavior resembles the redox properties of typical conductive films such as polypyrrole,[25] polyaniline,[27,28] or polythiophene.[29−31] The reduction and reoxidation of the Fc-C_{60}/Pd film involves cation transport between the film and the solution. The process can be described by the following reaction (reaction 1):

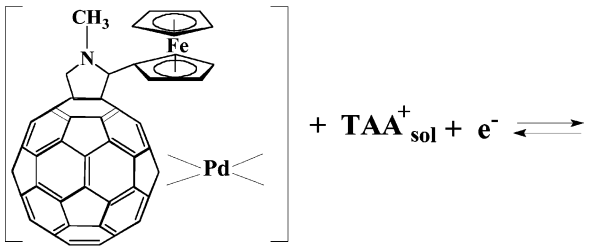

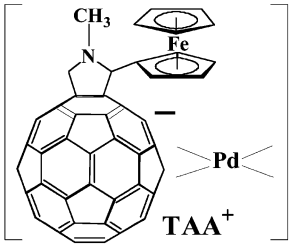

The oxidation of ferrocene groups occurs at positive potentials. This process resembles behavior observed for other redox-polymers.[59] The film oxidation peak is sharp and symmetrical. In contrast to the reduction process, the changes of film capacity associated with the oxidation process are much smaller. In this case, the electron transfer occurs via a process of sequential electron self-exchange between neighboring ferrocene groups. The charge percolation through the layer is accompanied by the anion transport between solution and the film according to the following reaction (reaction 2):

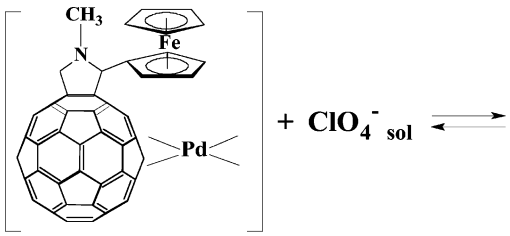

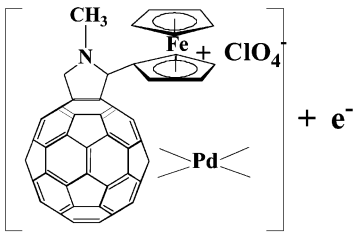

Depending on the film thickness and the sweep rate, the oxidation process can be controlled by the rate of electron transport (low sweep rate or thin film) or by the rate of ion transport (high sweep rate or thick film).

Under typical conditions, in acetonitrile solution containing tetra(*n*-alkyl)ammonium perchlorate as supporting electrolyte, the charge corresponding to the film oxidation process in the positive potential range is higher than the charge of film reduction at negative potentials. This behavior is related to higher permeability of the layer for the small perchlorate anions than large tetra(*n*-alkyl)ammonium cations. The oxidation process also results in substantial changes of the film structure.

A very strong effect of the composition of the growth solution on the process of film formation and the film redox properties is observed. This effect is probably related to the deposition of palladium nanoclusters along with the polymer on the electrode surface as was demonstrated for the C_{60}/Pd film previously.[40] The efficiency of palladium nanocluster formation increases with an increase in the palladium complex concentration in the growth solution.[40] Therefore, the charge associated with the oxidation process is low for these films, and reduction does not occur at all. Only the surface layer of the film is reversibly oxidized at positive potentials.

In the cathodic cycle following the film oxidation process, two reduction peaks, R_3' and R_3'', are observed in the voltammograms. Both arise from the reduction of oxidized ferrocene centers. The peak R_3' represents the reduction process described by reaction 2. The nature of peak R_3'' is more complex. In a previous paper we investigated the effect of the C_{60}/Pd film on the simple heterogeneous one-electron-transfer processes for selected redox systems.[41] We found that, in the case of the ferrocene$^{o/+}$ redox couple at a C_{60}/Pd coated electrode, the small and sharp surface peak is observed on voltammograms at potentials close to −750 mV in cathodic cycle, following the process of ferrocene oxidation. This peak is related to the interaction involving ferrocene cations and negatively charged C_{60}^- centers in the layer. Such interaction stabilizes the fullerene cation and shifts its reduction toward more negative potentials. The nature of R_3'' peak observed for Fc-C_{60}/Pd film seems to be very similar. The interaction between the positively charged ferrocene groups and C_{60}^- centers within the film may be responsible for the R_3'' peak formation. The presence of C_{60}^- centers even at relatively positive potentials is related to the partial reoxidation of the film in the anodic scan during film formation. If the film is relatively thick, the C_{60} sites buried deeply within the film are not reoxidized and remain negatively charged. The observation of infrared bands in the 3000−2900 cm^{-1} range due to the presence of tetra(*n*-butyl)ammonium cations in the film (see Figure 3) are consistent with the trapping of reduced fullerene moieties within the film. For thinner films, the reduction and oxidation process of the film in the negative potential range is completely reversible. This explains the fact that R_3'' peak is observed only on

(59) Dalton, E. F.; Surridge, N. A.; Jernigan, J. C.; Wilbourn, K. O.; Facci, J. S.; Murray, R. W. *Chem. Phys.* **1990**, *141*, 143.

voltammograms of relatively thick layers as shown in Figures7 and 11.

The results presented in this paper open a field of study of other transition metal complex Fc-C_{60} systems that may produce redox active films. The structure and properties of such films may be tuned by varying the chemical structure of the spacers connecting fullerene moieties. These films may have considerable potential in a number of applications. For example, they can be used as electron transfer mediators for both oxidation and reduction processes or as active materials for batteries and photovoltaic devices. The formation, structures, and redox properties of this family of electrochemically produced films are under investigation.

Acknowledgment. We thank Monika Turkowicz for the assistance in experiments. Financial support of the State Committee for Scientific Research, Poland, project 3 T09 A 182 19 (K.W.), National Science Foundation (grant CHE 0070291 to A.L.B.), and Gulbenkian Foundation for postdoctoral fellowship to A.dB.D. is gratefully acknowledged.

Supporting Information Available: Figure S1: Dependence of the peak current on sweep rate for the fullerene and ferrocene charge-transfer processes. Figure S2: Multicyclic voltammograms for film formation with varying concentrations of $[Pd(ac)_2]_3$. This material is available free of charge via the Internet at http://pubs.acs.org.

CM034364C